IOP Publishing Journal of Optics A: Pure and Applied Optics
J. Opt. A: Pure Appl. Opt. **9** (2007) S301–S307 doi:10.1088/1464-4258/9/9/S04

REVIEW ARTICLE

Metamaterials with negative permeability and negative refractive index: experiments and simulations

Ekmel Ozbay[1,2,3,4], **Kaan Guven**[1,2] **and Koray Aydin**[1,2]

[1] Nanotechnology Research Center, Bilkent University, Bilkent, 06800 Ankara, Turkey
[2] Department of Physics, Bilkent University, Bilkent, 06800 Ankara, Turkey
[3] Department of Electrical and Electronics Engineering, Bilkent University, Bilkent, 06800 Ankara, Turkey

E-mail: ozbay@bilkent.edu.tr and aydin@fen.bilkent.edu.tr

Received 31 January 2007, accepted for publication 19 April 2007
Published 22 August 2007
Online at stacks.iop.org/JOptA/9/S301

Abstract
We report the transmission characteristics of split-ring resonator and left-handed metamaterials (LHM) in the microwave frequency regime. A left-handed transmission band is observed at the frequencies where both dielectric permittivity and magnetic permeability are negative. The reflection characteristics of ordered and disordered LHMs are studied. The two-dimensional LHM structure is verified to have a negative refractive index. We employed three different methods to observe negative refraction: the beam shift method, refraction through wedge-shaped negative-index metamaterial, and phase-shift experiments.

Keywords: metamaterial, left-handed material, split-ring resonator, negative permeability, negative refraction, negative phase velocity, disorder, impedance matching

(Some figures in this article are in colour only in the electronic version)

1. Introduction

Metamaterials have become a remarkable research area in recent years and have received burgeoning interest due to their unprecedented properties that are unattainable from ordinary materials. Veselago pointed out that a material exhibiting negative values of dielectric permittivity (ε) and magnetic permeability (μ) would have a negative refractive index [1]. Generally speaking, dielectric permittivity (ε) and magnetic permeability (μ) are both positive for natural materials. In fact, it is possible to obtain negative values for ε and μ by utilizing appropriate designs of metamaterials. To be specific, negative permittivity values at microwave frequencies are accessed by making use of thin metallic wire meshes [2]. It is rather difficult to obtain negative permeability due to the absence of magnetic charges. Pendry *et al* developed a novel design consisting of two concentric rings with a split on each ring. This structure is called the split-ring resonator (SRR), since it exhibits a certain magnetic resonance at a certain frequency. An array of SRRs is then demonstrated to have negative permeability close to the resonance frequency [3]. The first steps to realizing these novel types of materials were taken by Smith *et al*, where they were able to observe a left-handed propagation band at frequencies where the dielectric permittivity and magnetic permeability of the composite metamaterial are negative [4, 5]. Soon after, left-handed metamaterials with an effective negative index of refraction were successfully demonstrated by various groups [6–9]. Negative refraction is also achieved by using periodically modulated two-dimensional photonic crystals [10].

One of the most exciting applications of negative-index metamaterials (NIM) is a perfect lens [11]. Stimulated by J B Pendry's seminal work, superlenses that are capable of imaging subwavelength-size objects have attracted a great deal

[4] Author to whom any correspondence should be addressed.

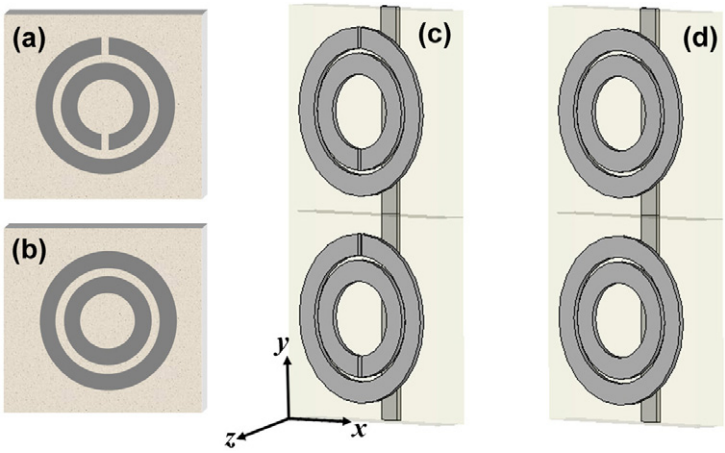

Figure 1. Schematic drawing of (a) a single split-ring resonator (SRR), (b) a closed-ring resonator (CRR), (c) a layer of a one-dimensional left-handed metamaterial (LHM) composed of SRR and wire arrays, and (d) a layer of one-dimensional composite material (LHM) composed of CRR and wire arrays.

of interest [12–20]. Sub-diffraction free imaging has been demonstrated experimentally for photonic crystals [12], left-handed transmission lines [13], and left-handed metamaterials (LHM) [14–16]. In the near-field regime, the electrostatic and magnetostatic limits apply and thus the electric and magnetic responses of materials can be treated as being decoupled. This, in turn, brings forth the possibility of constructing superlenses from materials with negative permittivity [17–19] or negative permeability [20]. Metamaterials offer a wide range of exciting physical phenomena that are not attainable with ubiquitous materials. To be specific, it has recently been shown that one can achieve cloaking by using metamaterial coatings [21, 22]. Metamaterial structures have recently been used to obtain novel mechanisms in nonlinear optics [23], and to increase the performance of active devices [24, 25]. Metamaterials are geometrically scalable, and therefore they offer a wide range of operating frequencies including radio [26], microwave [27–34], millimetre-wave [35], far-infrared (IR) [36], mid-IR [37, 38], near-IR [39, 40] frequencies, and even visible wavelengths [41, 42]. Recently, an acoustic analogue to electromagnetic metamaterials, the so-called ultrasonic metamaterials, was demonstrated [43].

In the present study, we demonstrate metamaterials with negative permeability and negative refractive index at microwave frequencies. Transmission and reflection measurements are performed to characterize these structures. We further investigated the disorder effects on performance metamaterials. We present the results of three independent refractive-index measurements that verify a negative index of refraction for the NIM structure under investigation. The refractive index values obtained from the three measurements are in good agreement.

2. Negative permeability metamaterials

2.1. Resonances of split-ring resonators

The response of materials to an incident magnetic field is determined by magnetic permeability. Magnetic permeability is positive in common materials. The absence of the negative values of magnetic permeability has provided little motivation for studying negative-index materials. Pendry *et al* proposed split-ring resonator (SRR) structures for obtaining negative permeability values [2]. The resonant behaviour of SRRs is due to the capacitive elements (gaps and splits), which in turn results in rather high positive and negative values of permeability near the magnetic resonance frequency (ω_{m}). The resonance characteristics of SRRs are studied in the literature in order to understand the mechanism behind negative permeability [44–48]. The split-ring resonators under investigation are built from concentric metal rings on a dielectric printed circuit board with a thickness of 1.6 mm and $\varepsilon = 3.85$. A schematic drawing of a split-ring resonator is shown in figure 1(a). The width of the splits and the gap between the inner and outer rings are 0.2 mm, the metal width is 0.9 mm, and the outer radius is 3.6 mm. The deposited metal is copper with a thickness of 30 μm. We also fabricated a ring resonator structure in which the splits are removed. The resulting structure is conventionally called a closed-ring resonator (CRR) and is shown schematically in figure 1(b).

We first measured the frequency response of the single split-ring resonator and closed-ring resonator unit cells. Two monopole antennae were used to transmit and detect the electromagnetic (EM) waves through the single SRR unit [47]. Monopole antennae were then connected to the HP-8510C network analyser for measuring the transmission coefficients. The measured frequency responses of a single SRR (blue solid line) and a single CRR (green solid line) are shown in figure 2. As seen in the figure, three transmission dips were observed at the frequencies 3.82, 8.12, and 10.90 GHz throughout the transmission spectrum of a single SRR. On the other hand, a single dip was observed at 10.92 GHz for a single CRR. We also performed simulations to compare with the experimental results. Simulations were performed by using the commercial software CST Microwave Studio, which is a three-dimensional (3D) full-wave solver that employs the finite integration technique. The simulated frequency responses of SRR (red dashed–dotted line) and CRR (grey dashed–dotted line) are shown in figure 2. The simulations are in good agreement with the experiments.

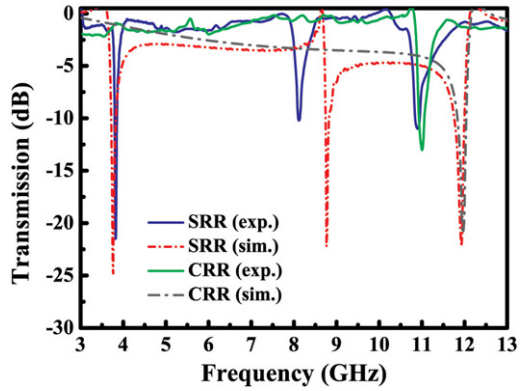

Figure 2. Measured and simulated frequency responses of single SRR and CRR structures.

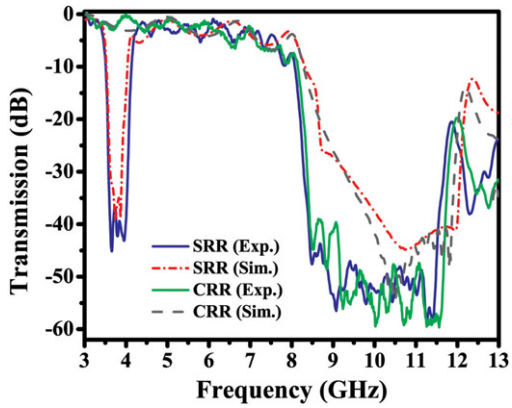

Figure 3. Measured and simulated transmission spectra of SRR and CRR arrays.

The splits in the split-ring resonators structure play a key role in attaining magnetic resonance. Removing the splits prevents the current from flowing between the inner and outer rings, and therefore the magnetic resonance is no longer present. Based on this principle, we observed two magnetic resonances for a split ring resonator structure at $\omega_{m1} = 3.82$ GHz and $\omega_{m2} = 8.12$ GHz. Recent studies have shown that it is possible to obtain tunable metamaterials by loading an SRR with varactors [49, 50] or capacitors [51]. By changing the capacitance in the capacitive regions of SRRs, the magnetic resonance frequency can successfully be changed.

A split-ring resonator not only exhibits magnetic resonance induced by the splits at the rings, but electric resonance is also present via the dipole-like charge distribution along the incident electric field [29, 30]. Such an electric resonance behaviour is observed at $\omega_e = 10.90$ GHz for the split-ring resonator and closed-ring resonator unit cells.

2.2. Split-ring resonator arrays

In section 2.1 we studied the frequency response of single SRR and CRR unit cells. If these structures are combined together, the coupling between the resonators results in band gaps around the resonance frequencies. To obtain negative permeability, we arranged SRR structures periodically. The number of unit cells along the x, y, and z directions are $N_x = 10$, $N_y = 15$, and $N_z = 25$, with lattice spacings $a_x = a_y = 8.8$ mm and $a_z = 6.5$ mm. The directions can be seen in figure 1(c). The wavevector is along the x direction, while the electric field (E-field) is along the y direction and the magnetic field (H-field) is along the z direction. The experimental setup for measuring the transmission amplitude and transmission phase spectra consists of an HP 8510C network analyser and standard high-gain microwave horn antennae [29]. Figure 3 shows the measured and simulated transmission spectra of periodic SRRs and CRRs. The first band gap between 3.55–4.05 GHz was observed at the transmission spectrum of the SRR array but not in the CRR array. However, the second band gap between 8.15–11.95 GHz was observed for both cases. As is clearly seen in the figure, the agreement between the measured and simulated data is good.

Based on the measurements and simulations, we can safely claim that the stop bands of split-ring resonator media cannot be assumed to be the result of 'negative μ' behaviour. Some of the observed gaps (such as the second band gap in this measurement) in the transmission spectra could also have originated from the electrical response from the split-ring resonators or from Bragg gaps due to periodicity [29]. The band gap between 3.55–4.05 GHz is due to the magnetic response of split-ring resonators. However, the stop band 8.15–11.95 GHz appeared due to the electrical response from the concentric rings.

3. Left-handed metamaterial

3.1. Left-handed transmission band

The LHM that is studied in this work consists of a periodic arrangement of SRR and thin wire arrays. Split-ring resonator and wire patterns are fabricated on the front and back sides of FR4 printed circuit boards, respectively. A schematic drawing of a sample is provided in figure 1(c). The length and width of the continuous thin wire structures are $l = 19$ cm and $w = 0.9$ mm. The left-handed material is composed of $N_x = 5$, $N_y = 15$, and $N_z = 32$ unit cells, with lattice spacings $a_x = a_y = 8.8$ mm and $a_z = 6.5$ mm [29]. Note that the lattice spacings were kept the same as the lattice spacing of the only split-ring resonator medium studied in section 2.

Figure 4(a) depicts the measured transmission spectra of SRR (blue line), LHM (red line), and a composite metamaterial (CMM) composed of CRR and wire arrays (black line) with five unit cells along the propagation direction. The band gap in the transmission spectrum of the SRR between 3.55 and 4.05 GHz was shown to be due to the magnetic resonance in section 2, and therefore the effective magnetic permeability is negative within this frequency range. Negative permittivity is satisfied by using thin metallic wire meshes [2]. The plasma frequency of the wire array that is used to construct the left-handed material in the present study is shown to be 8.0 GHz in a previous study [29]. Therefore, below 8.0 GHz, the effective permittivity of a wire array is negative. The condition for the formation of a left-handed transmission band is that the effective ε and μ should be simultaneously negative at a particular frequency range. As seen in figure 4(a), a transmission band (shaded region in the figure) is observed between 3.55–4.05 GHz. The transmission peak is measured to

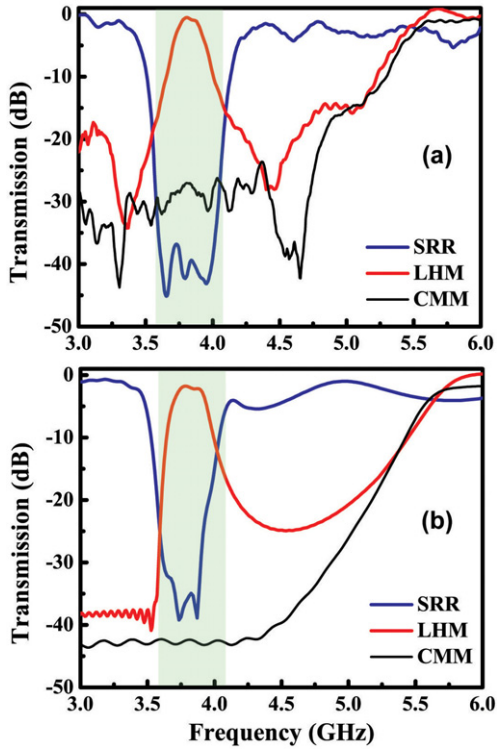

Figure 4. Transmission spectra of periodic SRR (blue line), LHM (red line), and CMM (black line) arrays obtained from (a) measurements and (b) numerical simulations. The shaded regions correspond to the left-handed propagation regime.

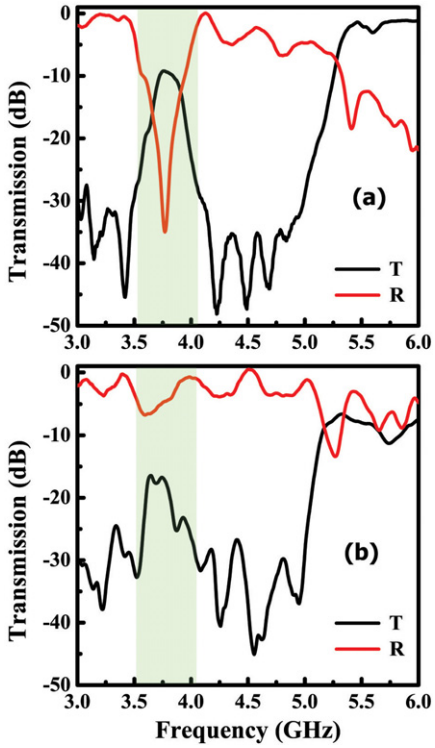

Figure 5. Measured transmission (black line) and reflection (red line) spectra of ten-layer (a) ordered and (b) disordered LHM structures.

be −0.8 dB at 3.86 GHz. This is the highest transmission peak measured for a LHM structure. For the composite metamaterial of CRR and wire arrays, the transmission band disappeared. We indicated that the wire media has a plasma frequency of approximately 8 GHz. SRR and CRR structures also have electric responses, and therefore contribute to the total electric response of the composite systems (LHM and CMM). The resulting LHM has a plasma frequency of approximately 5.4 GHz, and therefore the plasma frequency is reduced [29]. We performed numerical simulations in order to check the validity of the experimental results. The numerical simulation results are provided in figure 4(b) and predict a left-handed transmission band with a peak value of −2.7 dB between 3.60 and 4.10 GHz.

3.2. Reflection characteristics of 1D double negative material

In this section we present the reflection measurements of a one-dimensional (1D) LHM structure. In the measurements, the transmitter and receiver horn antennae were placed close to each other by keeping the angle between the antennae very small. The transmitter horn antenna sends the EM wave to the first surface of the structures, and the receiver antenna measures the amplitude of the reflected EM waves. The number of layers along the propagation direction is $N_x = 10$ layers in the present study. Figure 5(a) shows the measured transmission (black line) and reflection (red line) spectra. The transmission peak is −9.2 dB at 3.76 GHz. As was expected, as the number of layers along the propagation direction increases, the transmission within the left-handed transmission band decreases due to the losses.

In the reflection spectrum, a sharp dip with a minimum value of −35 dB is observed at 3.77 GHz. The incident EM waves with frequencies at approximately 3.77 GHz are nearly transmitted through the left-handed material without being reflected at the left-handed material–air interface. The low reflection from the surface can be attributed to either matched impedance at the interface or the thickness resonance of the slab. In a recent study, we showed, by extracting the effective parameters using a retrieval procedure, that the impedance is matched to free space [52]. Impedance matching is desired for NIM structures, since it is required to achieve a perfect lens [11].

3.3. Effect of disorders on transmission and reflection

We investigated the transmission and reflection properties of ordered left-handed materials. In this section we discuss the effect of disorder on the transmission and reflection characteristics. The transmission characteristics of disordered left-handed materials are investigated in detail [53–55]. The effects of disorder need to be investigated to determine the restrictions imposed on the impedance matching of LHMs. For this purpose, we introduced disorder into the LHM system by randomly destroying the periodicity of a split-ring resonator array along the x and y directions. The disorder is introduced as follows: each split-ring resonator on the board with lattice point $\mathbf{r}_n$, where $\mathbf{r} = x\hat{\mathbf{i}} + y\hat{\mathbf{j}}$, is displaced by $\mathbf{r}_n \pm \boldsymbol{\delta}_r$. Here $\boldsymbol{\delta}_r$ is the randomness parameter, which we chose to be $|\boldsymbol{\delta}_r| = a/9$, where $a = a_x = a_y = 8.8$ mm is the lattice constant of the periodic SRR array. Then the disordered LHM is obtained by

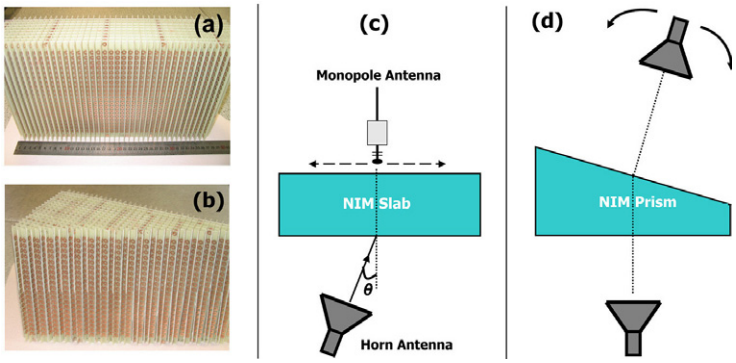

Figure 6. Photographs of (a) a ten-layer NIM slab and (b) a wedge-shaped NIM. Scheme of experimental setups for verifying negative refraction by using the (c) beam-shift method, and (d) wedge experiments.

arranging disordered split-ring resonator arrays with ordered wire arrays with the same number of unit cells along all directions [53].

Figure 5(b) plots the transmission (black line) and the reflection (red line) spectra of a disordered left-handed material array. There is a significant amount of reduction in the transmission peak. The peak value is −16.1 dB and the transmission band becomes narrower. A wider reflection band is observed where the minimum value of the reflection is approximately −7 dB. A sharp dip, as in the case of ordered left-handed materials, was not observed. It is obvious that the disorders affect the reflection and transmission properties of LHMs. They affect the coupling between the SRRs and wires, and therefore the resulting left-handed materials' characteristics are changed. The periodicity is important in order to achieve high transmission and low reflection from a left-handed metamaterial.

4. Negative refraction

In the previous two sections we performed transmission and reflection measurements to characterize the split-ring resonators and left-handed metamaterials. In this section we move on to the experiments to measure the refractive index of our sample in the left-handed frequency region. We performed three different and independent experimental measurements to verify that the index of refraction is negative. First, we measured refraction through a 2D left-handed material slab by using the beam-shift method. We also performed refraction experiments on wedge-shaped samples. Finally, we performed a phase-shift experiment to verify and calculate the negative refractive index.

4.1. Refraction through slab-shaped left-handed materials

The 2D left-handed material is composed of $N_x = 10$, $N_y = 20$ and $N_z = 40$ unit cells, with lattice spacings $a_x = a_y = a_z = 9.3$ mm, as seen in figure 6(a) [56]. The refraction spectrum is measured using a setup consisting of a microwave horn antenna as the transmitter and a monopole antenna as the receiver (see figure 6(c)). The incident EM wave hits the air–left-handed material interface with an angle of $\theta_i = 15°$. The source is 12 cm (1.5λ) away from the first interface of the NIM slab. The spatial intensity distribution along the second NIM–air interface is scanned in $\Delta x = 2.5$ mm steps.

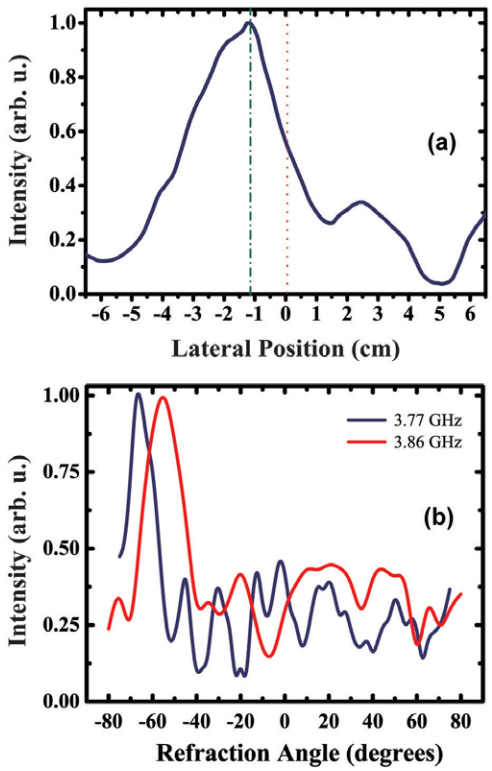

Figure 7. (a) Measured refracted beam profile on the exit surface of an NIM slab at 3.86 GHz. The centre of the refracted beam is shifted to the left, meaning in turn that the effective refractive index is negative. (b) The measured beam profiles from the waves refracted from a wedge-shaped 2D left-handed material at 3.77 GHz (blue line) and 3.86 GHz (red line).

Figure 7(a) displays the refracted beam profile at 3.86 GHz. The centre of the refracted Gaussian beam is measured −1.25 cm away from the centre of the incident Gaussian beam. Note that the incident EM wave has a Gaussian beam profile centred at $x = 0$ (not shown in the figure). One can easily find the refractive index value by applying Snell's law, where $n_{air} \sin\theta_i = n_{LHM} \sin\theta_r$. The angle of refraction can be defined in terms of the beam shift

(d_s) and width of the left-handed material slab (w) as $\theta_r = \arctan(d_s/w)$. The effective refractive index of the NIM is then calculated as $n_{eff} = -1.91$ at 3.86 GHz [56].

4.2. Refraction through wedge-shaped left-handed materials

A typical experimental method for the observation of left-handed properties is to use wedge-shaped structures [6–9]. We constructed a wedge-shaped left-handed material with a wedge angle of $\theta = 26°$, as shown in figure 6(b). The first interface of left-handed material is excited with EM waves emanating from the transmitter horn antenna that is located at a distance of 13 cm ($\sim 2\lambda$) away from the first interface of the wedge. The receiver horn antenna is placed 70 cm ($\sim 10\lambda$) away from the second interface of the wedge-shaped NIM. It is mounted on a rotating arm in order to scan the angular distribution of the refracted signal. The angular refraction spectrum is scanned with a $\Delta\theta = 2.5°$ step size. A scheme of the experimental setup is provided in figure 6(d).

The refracted beam profiles from the NIM–air interface are shown in figure 7(b) for two different frequencies: 3.77 GHz (blue line) and 3.86 GHz (red line). At these frequencies, the beam is refracted on the negative side of the normal, indicating that the angle of refraction is negative. The angle of refraction at 3.77 GHz is $\theta_r = -65°$ and at 3.86 GHz it is $\theta_r = -60°$. We can use Snell's law for calculating the n_{eff} of the 2D NIM structure using the simple formula $n_{eff} \sin\theta_i = n_{air} \sin\theta_r$. At 3.86 GHz the refractive index is calculated as $n_{eff} = -1.98 \pm 0.05$. The angle of refraction increases when the frequency is lowered, hence n_{eff} increases. The calculated refractive index at 3.77 GHz is $n_{eff} = -2.07 \pm 0.05$.

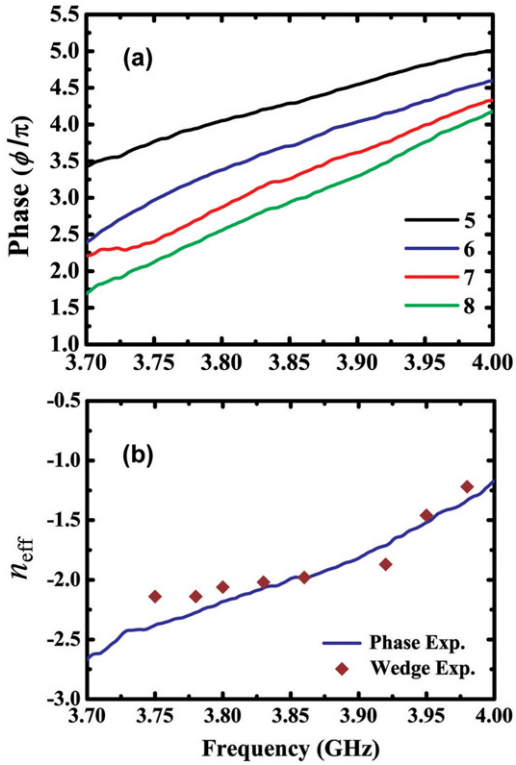

Figure 8. (a) The measured transmission phase spectra of five to eight layers of LHM structures. The phase decreases with an increasing number of layers along the propagation direction. (b) Measured effective refractive indices as a function of frequency. The results obtained from the phase-shift experiments (blue line) and wedge experiments (♦) are in good agreement.

5. Negative phase velocity

For materials with a negative refractive index, the phase velocity points toward the source, that is, the phase velocity and energy flow are anti-parallel inside a NIM [9, 57, 58]. By measuring the transmission phases for NIMs with varying thicknesses, one can verify that the phase velocity is indeed negative. An HP 8510-C network analyser is capable of measuring the transmission phase. We have constructed four different 2D NIM slabs with a number of layers $N_x = 5, 6, 7,$ and 8. The transmitted phases are plotted in the frequency range 3.70–4.00 GHz, which is within the left-handed transmission region.

Figure 8(a) shows the transmitted phase for the different numbers of layers in the NIM slabs. It is evident from the figure that increasing the number of layers in the NIM results in a decrease in the phase of the transmitted EM wave. However, if the material possesses a positive refractive index, one would observe an increase in the transmitted phase with an increasing number of unit cells [9, 59].

The index of refraction in terms of wavelength, phase shift, and the change in the length of the left-handed material is given by [9]:

$$n = \frac{\Delta\phi}{\Delta L}\frac{\lambda}{2\pi}. \quad (1)$$

At $f = 3.86$ GHz, the wavelength of the EM wave is $\lambda = 7.77$ cm. The average phase shift per unit cell ($\Delta L = 8.8$ mm) obtained from the experimental results is $\Delta\Phi = -0.45 \pm 0.04\pi$. Inserting these values in (1), the index of refraction at 3.86 GHz is found to be $n_{eff} = -1.98 \pm 0.18$. The average phase shift and calculated refractive index for the numerical simulations at 3.77 GHz are $\Delta\Phi = -0.51 \pm 0.04\pi$ and $n_{eff} = -2.31 \pm 0.18$.

In figure 8(b), we plotted the refractive index values calculated by using the phase shift between the consecutive numbers of NIM layers. The symbol (♦) corresponds to the refractive indices obtained from wedge experiments at some other frequencies (data not shown here). There is good agreement between the results obtained from the two different methods. We also found the index of refraction at 3.86 GHz using the beam-shift method as -1.91. The index of refraction values obtained from the wedge and the phase-shift experiment are both -1.98 at this frequency. Therefore, we have been able to show that the results obtained from three different experiments agree extremely well.

6. Conclusion

In conclusion, we have successfully demonstrated a left-handed transmission band for a 1D double negative material in free space with a high transmission peak. Magnetic resonances of split-ring resonator structures are verified by using a closed-ring resonator structure. The effect of disorder on the transmission and reflection characteristics of 1D double negative materials is studied experimentally. We confirmed

that a 2D negative-index metamaterial has a negative refractive index at frequencies where the dielectric permittivity and magnetic permeability are simultaneously negative. We were able to observe a negative refractive index for 2D NIMs by using three different independent methods. The results obtained from these experiments are in good agreement. The phase shift, and therefore the phase velocity, is shown to be negative.

Acknowledgments

This work is supported by the European Union under the projects EU-NoE-METAMORPHOSE and EU-NoE-PHOREMOST, and by TUBITAK (The Scientific and Technological Research Council of Turkey) under projects nos 104E090, 105E066, 105A005, and 106A017. One of the authors (EO) also acknowledges partial support from the Turkish Academy of Sciences.

References

[1] Veselago V G 1968 *Sov. Phys.—Usp.* **10** 509
[2] Pendry J B, Holden A J, Robbins D J and Stewart W J 1998 *J. Phys.: Condens. Matter* **10** 4785
[3] Pendry J B, Holden A J, Robbins D J and Stewart W J 1999 *IEEE Trans. Microw. Theory Tech.* **47** 2075
[4] Smith D R, Padilla W J, Vier D C, Nemat-Nasser S C and Schultz S 2000 *Phys. Rev. Lett.* **84** 4184
[5] Shelby R A, Smith D R, Nemat-Nasser S C and Schultz S 2001 *Appl. Phys. Lett.* **78** 480
[6] Shelby R A, Smith D R and Schultz S 2001 *Science* **292** 77
[7] Parazzoli C G, Greegor R B, Li K, Koltenbah B E and Tanielian M 2003 *Phys. Rev. Lett.* **90** 107401
[8] Houck A A, Brock J B and Chuang I L 2003 *Phys. Rev. Lett.* **90** 137401
[9] Aydin K, Guven K, Soukoulis C M and Ozbay E 2005 *Appl. Phys. Lett.* **86** 124102
[10] Cubukcu E, Aydin K, Ozbay E, Foteinopoulou S and Soukoulis C M 2003 *Nature* **423** 604
[11] Pendry J B 2000 *Phys. Rev. Lett.* **85** 3966
[12] Cubukcu E, Aydin K, Ozbay E, Foteinopolou S and Soukoulis C M 2003 *Phys. Rev. Lett.* **91** 207401
[13] Grbic A and Eleftheriades G V 2004 *Phys. Rev. Lett.* **92** 117403
[14] Lagarkov A N and Kissel V N 2004 *Phys. Rev. Lett.* **92** 077401
[15] Aydin K, Bulu I and Ozbay E 2005 *Opt. Express* **13** 8753
[16] Aydin K, Bulu I and Ozbay E 2006 *New J. Phys.* **8** 221
[17] Fang N, Lee H, Sun C and Zhang X 2005 *Science* **308** 534
[18] Melville D O S and Blaikie R J 2005 *Opt. Express* **13** 2127
[19] Taubner T, Korobkin D, Urzhumov Y, Shvets G and Hillenbrand R 2006 *Science* **313** 1595
[20] Guven K and Ozbay E 2006 *Opto-Electron. Rev.* **14** 213
[21] Pendry J B, Schurig D and Smith D R 2006 *Science* **312** 1780
[22] Schurig D, Mock J J, Justice B J, Cummer S A, Pendry J B, Starr A F and Smith D R 2006 *Science* **314** 977
[23] Klein M W, Enkrich C, Wegener M and Linden S 2006 *Science* **313** 502
[24] Padilla W J, Taylor A J, Highstrete C, Lee M and Averitt R D 2006 *Phys. Rev. Lett.* **96** 107401
[25] Chen H, Padilla W J, Zide J M O, Gossard A C, Taylor A J and Averitt R D 2006 *Nature* **444** 597
[26] Wiltshire M C K, Pendry J B, Young I R, Larkman D J, Gilderdale D J and Hajnal J V 2001 *Science* **291** 849
[27] Bayindir M, Aydin K, Markos P, Soukoulis C M and Ozbay E 2002 *Appl. Phys. Lett.* **81** 120
[28] Ziolkowski R W 2003 *IEEE Trans. Antennas Propag.* **51** 1516
[29] Aydin K, Guven K, Kafesaki M, Zhang L, Soukoulis C M and Ozbay E 2004 *Opt. Lett.* **29** 2623
[30] Katsarakis N, Koschny T, Kafesaki M, Economou E N and Soukoulis C M 2004 *Appl. Phys. Lett.* **84** 2943
[31] Bulu I, Caglayan H, Aydin K and Ozbay E 2005 *New J. Phys.* **7** 223
[32] Bulu I, Caglayan H and Ozbay E 2005 *Opt. Express* **13** 10238
[33] Gundogdu T F, Tsiapa I, Kostopoulos A, Konstantinidis G, Katsarakis N, Penciu R S, Kafesaki M, Economou E N, Koschny T and Soukoulis C M 2006 *Appl. Phys. Lett.* **89** 084103
[34] Guven K, Caliskan M D and Ozbay E 2006 *Opt. Express* **14** 8685
[35] Gokkavas M, Guven K, Bulu I, Aydin K, Penciu R S, Kafesaki M, Soukoulis C M and Ozbay E 2006 *Phys. Rev.* B **73** 193103
[36] Yen T J, Padilla W J, Fang N, Vier D C, Smith D R, Pendry J B, Basov D N and Zhang X 2004 *Science* **303** 1494
[37] Linden S, Enkrich C, Wegener M, Zhou J, Koschny T and Soukoulis C M 2004 *Science* **306** 1351
[38] Moser H O, Casse B D F, Wilhelmi O and Saw B T 2005 *Phys. Rev. Lett.* **94** 063901
[39] Shalaev V M, Cai W, Chettiar U K, Yuan H, Sarychev A K, Drachev V P and Kildishev V 2005 *Opt. Lett.* **30** 3356
[40] Zhang S, Fan W, Panoiu N C, Malloy K J, Osgood R M and Brueck S R J 2005 *Phys. Rev. Lett.* **95** 137404
[41] Grigorenko A N, Geim A K, Gleeson H F, Zhang Y, Firsov A A, Khrushchev I Y and Petrovic J 2005 *Nature* **438** 335
[42] Dolling G, Wegener M, Soukoulis C M and Linden S 2007 *Opt. Lett.* **32** 53
[43] Fang N, Xi D, Xu J, Ambati M, Srituravanich W, Sun C and Zhang X 2006 *Nat. Mater.* **5** 452
[44] Weiland T, Schuhmann R, Greegor R B, Parazzoli C G, Vetter A M, Smith D R, Vier D C and Schultz S 2001 *J. Appl. Phys.* **90** 5419
[45] Gay-Balmaz P and Martin O J F 2002 *J. Appl. Phys.* **92** 2929
[46] Marques R, Mesa F, Martel J and Medina F 2003 *IEEE Trans. Antennas Propag.* **51** 2572
[47] Aydin K, Bulu I, Guven K, Kafesaki M, Soukoulis C M and Ozbay E 2005 *New J. Phys.* **7** 168
[48] Aydin K and Ozbay E 2006 *Opto-Electron. Rev.* **14** 193
[49] Gil I, Garcia-Garcia J, Bonache J, Martin F, Sorolla M and Marques R 2004 *Electron. Lett.* **40** 1347
[50] Shadrivov I V, Morrison S K and Kivshar Y S 2006 *Opt. Express* **14** 9344
[51] Aydin K and Ozbay E 2007 *J. Appl. Phys.* **101** 024911
[52] Aydin K, Bulu I and Ozbay E 2006 *Microw. Opt. Technol. Lett.* **48** 2548
[53] Aydin K, Guven K, Katsarakis N, Soukoulis C M and Ozbay E 2004 *Opt. Express* **12** 5896
[54] Gorkunov M V, Gredeskul S A, Shadrivov I V and Kivshar Y S 2006 *Phys. Rev.* E **73** 056605
[55] Guven K, Aydin K and Ozbay E 2005 *Photonics Nanostruct.: Fund. Appl.* **3** 75
[56] Aydin K and Ozbay E 2006 *J. Opt. Soc. Am.* B **23** 415
[57] Cummer S A and Popa B 2004 *Appl. Phys. Lett.* **85** 4564
[58] Dolling G, Enkrich C, Wegener M, Soukoulis C M and Linden S 2006 *Science* **312** 892
[59] Aydin K and Ozbay E 2007 *Appl. Phys.* A **87** 137